

Why are mixed-phase altocumulus clouds poorly predicted by large-scale models? Part I: Physical processes

Andrew I. Barrett,¹ Robin J. Hogan¹ and Richard M. Forbes²

Abstract. Stratiform mixed-phase clouds are poorly simulated by current weather forecast and climate models causing erroneous predictions of radiative transfer. Five operational models and ERA-Interim reanalyses were evaluated using ground-based remote sensors. All models underestimated the supercooled liquid water content by at least a factor of 2. Models with the most sophisticated microphysics (separate prognostic variables for liquid and ice) performed worst, having least supercooled liquid of all models. To investigate the reason for this, a new single column model (EMPIRE) has been developed, with high vertical resolution and a non-local turbulent mixing scheme, which was able to simulate persistent mixed-phase clouds similar to those observed. Large sensitivities were found to ice microphysics and vertical resolution, with smaller sensitivities to the frequency of radiation scheme calls, turbulent mixing specification and the critical relative humidity at which cloud forms. In particular, any microphysical change that reduces the ice growth rate results in increased cloud lifetime and liquid water content. Using aircraft data we demonstrate the importance of the ice particle size distribution intercept parameter, N_0 , increasing with increasing ice water content. Compared to the default fixed N_0 , this significantly improves the persistence of supercooled water. A large sensitivity to the vertical resolution of the model is also found; a sub-grid parameterization for models with coarse vertical resolution is proposed in Part II.

1. Introduction

Stratiform mixed-phase altocumulus clouds are not well simulated by current weather forecast models (and by extension climate models) resulting in erroneous predictions of radiative transfer. The liquid-over-ice vertical structure of mixed-phase clouds [Hobbs and Rangno, 1985; Rauber and Tokay, 1991], their large areal extent and long lifetime [Shupe *et al.*, 2008; Morrison *et al.*, 2012] means they are a significant contributor to the cloud radiative effect. The liquid layer at cloud top consists of a large concentration of small droplets with effective radii as small as $2\ \mu\text{m}$ [Hogan *et al.*, 2003] and is effective at reflecting solar radiation incident on the cloud. Correctly predicting the phase of the cloud condensate is therefore important for calculating the radiative impact of mixed-phase clouds.

The different radiative properties of liquid and ice clouds is the reason for the large sensitivity to mixed-phase cloud specification found in GCMs [e.g. Mitchell *et al.*, 1989; Senior and Mitchell, 1993; Sun and Shine, 1994; Gregory and Morris, 1996]. However, the magnitude of such changes are uncertain given the basic state of the cloud physics used in these studies. Calculations of the radiative impact of mixed-phase clouds by Hogan *et al.* [2003] showed that the supercooled liquid water layer at cloud top dominated the overall radiative impact of the cloud, strongly increasing the amount of reflected short wave radiation while only slightly decreasing the total outgoing long wave radiation. The net result was a reduction in the amount of radiation absorbed by the atmosphere. Sun and Shine [1994] calculated the radiative impact of three different cloud structures of liquid

and ice (uniformly mixed, horizontally stratified and horizontally adjacent), concluding that the impact of a uniformly mixed cloud was largest, but their horizontally stratified cloud was ice over liquid, opposite to that of mixed-phase altocumulus cloud.

Despite their potential radiative importance, cloud at mid-levels in the atmosphere tends to be underestimated by both numerical weather prediction (NWP) models [e.g. Illingworth *et al.*, 2007] and climate models [Zhang *et al.*, 2005] suggesting a deficiency in the representation of mixed-phase clouds. An absence of these mixed-phase clouds would likely result in excess solar radiation reaching the surface and excess longwave emission at the top of the atmosphere [e.g. Hogan *et al.*, 2003] which could result in a warm or cold bias at the surface depending on the time of day. The net cooling effect may not be captured by current models and this would constitute a missing negative feedback on the climate system in these models (as reported by Mitchell *et al.* [1989]) if the amount of polar and extra-tropical mid-latitude cloud increases as suggested by some studies [e.g. Tsushima *et al.*, 2006]. Cloud feedbacks are the largest single cause of inter-model variability in predicted climate scenarios during Coupled Model Intercomparison Project Phase 3 (CMIP3) [Bony *et al.*, 2006; Dufresne and Bony, 2008] and CMIP5 [Andrews *et al.*, 2012] and this is despite the mixed-phase cloud feedbacks likely being underestimated in many climate models.

Supercooled liquid-topped stratiform clouds have been observed at many latitudes from space-borne lidar. Hogan *et al.* [2004] reported that liquid water was detected at temperatures down to -35°C by the Lidar In-space Technology Experiment (LITE) and Zhang *et al.* [2010] detailed the global frequency of mid-level liquid-topped layer clouds finding local frequency of occurrence up to 15%. Extensive observations of mixed-phase clouds have been made in the Arctic (e.g. M-PACE [Verlinde *et al.*, 2007], SHEBA [Utter *et al.*, 2002], ISDAC [McFarquhar *et al.*, 2011]) that have been followed by a number of modelling studies. These studies found that both single-column and cloud-resolving models underestimate the liquid water content by a factor of 3 on

¹Department of Meteorology, University of Reading, UK.

²European Centre for Medium-Range Weather Forecasts, Reading, UK.

average [e.g. *Klein et al.*, 2009]. *Klein et al.* [2009] attributed this difference to errors in the production of ice. The liquid water content can be more realistically represented if the concentration of ice nuclei is included as a prognostic variable and therefore allows the ice nuclei to be depleted [*Fridlind et al.*, 2012]; however, this resulted in unrealistically low ice particle number concentrations. Maintaining persistent cloud layers with both liquid and ice concentrations close to observations remains a challenge.

At lower latitudes, thin mixed-phase clouds commonly exist at mid-levels in the form of altocumulus; these clouds have been less studied in the literature and have a potentially greater radiative impact owing to the lower solar zenith angle and darker surface over which they form. Although there may be differences to Arctic stratocumulus cloud, there are also many similarities in the structure and the processes that are relevant for the maintenance of cloud top supercooled liquid water layers [*Morrison et al.*, 2012]. This paper takes advantage of the long timeseries of ground-based remote-sensing observations at a mid-latitude location, Chilbolton in southern England, to focus on these mixed-phase clouds and understand which aspects of the model are most important for their representation and improved simulation.

Part I of the paper evaluates mixed-phase representation in a range of NWP and regional climate models using surface based remote-sensing observations and, by the application of a new single-column model, investigates which aspects of model configuration could lead to poor simulation of mixed-phase altocumulus. Part II addresses the model sensitivity to vertical resolution in more detail, determines where the sensitivity comes from and describes a novel parameterization suitable for large-scale models that can remove the sensitivity to vertical resolution.

In this paper, section 2 describes the model and remote-sensing data used, which is used to evaluate the mixed-phase cloud representation of current models in section 3. The EMPIRE model is described in section 4 and used in section 5 to determine which processes are most important to be represented correctly in the model. An evaluation of the importance of the ice particle size distribution specification using aircraft observations is presented in section 6, and conclusions are drawn in section 7.

2. Remote sensing and model data processing

2.1. Observational data and retrieval

The observational data used in this paper come from ground-based remote-sensing instrumentation (vertically pointing radar, lidar and microwave radiometer) based at Chilbolton in Southern England, which forms part of the Cloudnet research project [*Illingworth et al.*, 2007]. Observations from 2003 to 2009 were used to evaluate NWP models in section 3. Much of the raw data from the instruments has been combined and processed as part of the Cloudnet project. This includes quality control of the data, conversion of radar reflectivity, lidar backscatter and brightness temperatures to liquid and ice water contents and cloud fractions, averaging of the high resolution data to model grid scales and incorporation of model forecasts of temperature and pressure. An example of the process to combine these observations is shown in Figure 1 for an observed mixed-phase cloud on 2 April 2005 and a description of this process follows.

The radar reflectivity (Fig. 1a) and lidar backscatter (Fig. 1b) were used together with the radar Doppler velocity (not shown) to determine the nature of the target (target classification; Fig. 1c). The lidar is sensitive to the numerous small liquid droplets and the radar is most sensitive to the larger ice particles so it is possible to determine the phase of the target; this is aided by the radar Doppler velocity which highlights falling ice particles.

Where ice particles were detected, the ice water content within each pixel is determined using the empirical relationship from *Hogan et al.* [2006]. This empirical relationship was derived from aircraft observations; although this relationship was formulated on mid-latitude clouds which were not specifically mixed-phase it is anticipated that the ice falling from mixed-phase clouds will follow a similar relationship between ice water content and radar reflectivity to that derived by *Hogan et al.* [2006].

The liquid water content values were obtained through the use of all three instruments. The Cloudnet retrieval algorithm uses the lidar to identify the base of a liquid cloud layer, but due to the attenuation of the lidar beam by liquid water it is unable to detect the cloud top reliably, so instead the cloud top height derived from the radar is used. Using the cloud top and base height and model temperature and pressure, the liquid water content profile is calculated assuming that the cloud is adiabatic from cloud base to cloud top. The liquid water path (the vertical integral of the liquid water content) measured by the microwave radiometer (Fig. 1d) is then used to scale the in-cloud liquid water content profile. This method does not work well when multiple layers of cloud are present, as discussed further in section 2.2.

Once the liquid and ice water contents have been calculated on the high-resolution data (Fig. 1e,f), it is then averaged to the model grid scale. This involves averaging over height ranges consistent with the spacing of the model vertical levels and over sufficient time to represent the horizontal grid spacing of the model (calculated using the model horizontal wind speed). This is done separately for each model and therefore results in a number of different ‘observations’. The liquid and ice water contents are the observed mean in the vertical and horizontal (time) space corresponding to the model grid-box whereas the cloud fraction is the number of pixels where the liquid or ice water content is larger than zero. The cloud fraction is not split by phase in the Cloudnet data so the total cloud fraction is assumed to be that for ice cloud and the liquid cloud fraction was calculated using the same method as used to generate the total cloud fraction but counting the fraction of pixels which had a liquid water content greater than zero.

2.2. Selection of days

A study of the full climatology of mixed-phase clouds at Chilbolton would be ideal but obtaining reliable information about their structure from surface based remote sensors is difficult when low cloud is present. To detect a liquid layer in mid-level clouds the lidar signal must not be attenuated; however, low-level clouds are usually liquid-phase with an optical depth large enough to completely attenuate the lidar signal. Liquid water path measurements are needed to obtain the liquid water content within the cloud but, when multiple cloud layers exist, reliable estimates of the liquid water content in each layer can not be made. For this reason, only days with single-layer mid-level mixed-phase clouds were selected for analysis and only at times when there were no low level clouds; this restriction substantially reduces the number of days and times suitable for analysis relative to the number of days on which mixed-phase clouds occurred. Days that were suitable for part of the day were included, but only the parts of the day that fit the above criteria were included in the analysis.

This method gives us more useful information than a case study would, but is not as satisfactory as a full climatology. It is also possible that by selecting days where mixed-phase clouds were observed, but without using any information from the models, that the model data may be biased from

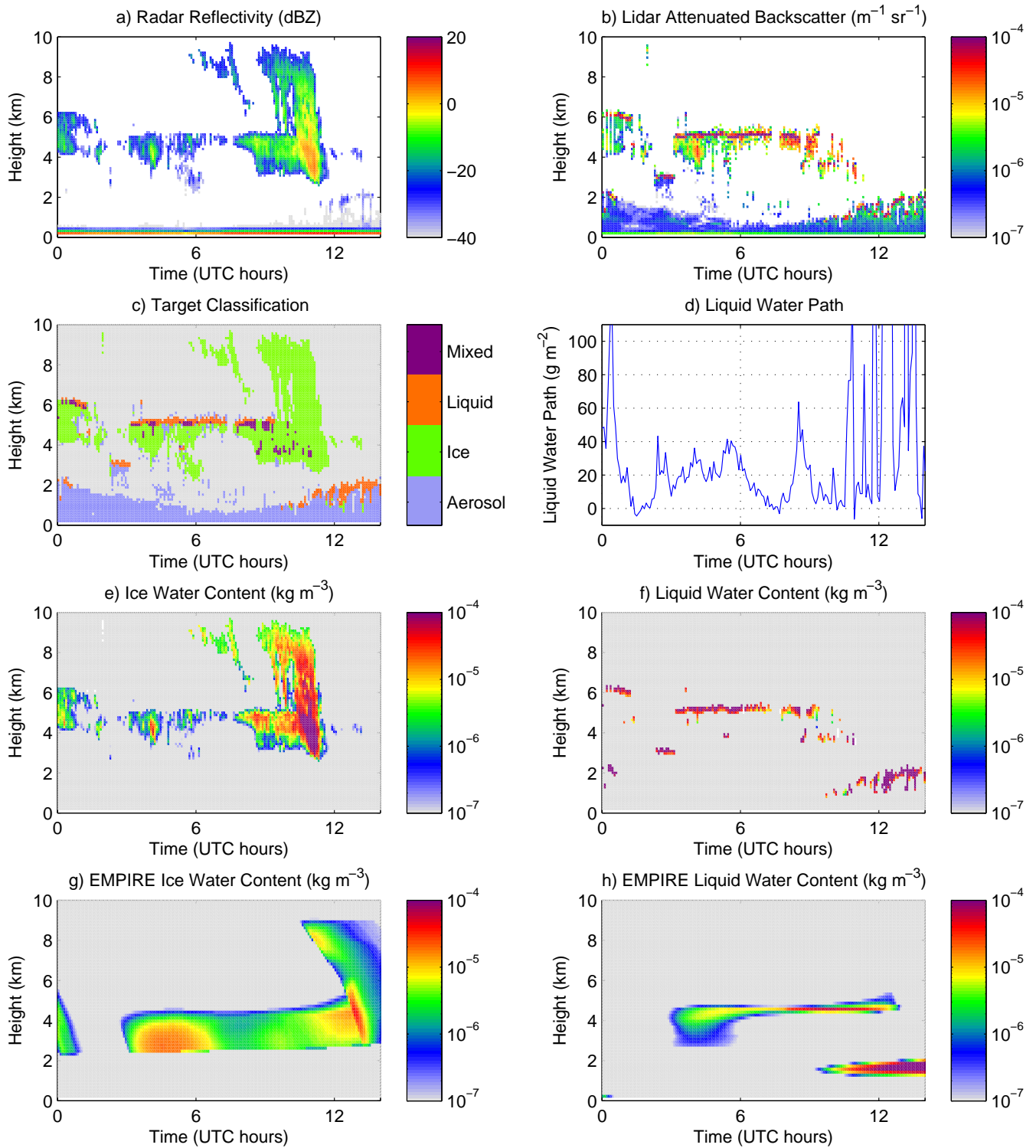


Figure 1. Illustration of the a) radar and b) lidar observations from 3 July 2003 at Chilbolton used together in c) to determine the target type. The liquid water path measured by the microwave radiometer is shown in d) and the derived ice and liquid water contents in e) and f). For comparison the EMPIRE model simulations of grid-box mean ice and liquid water contents are shown in g) and h).

that of a true climatology. After selecting suitable days and restricting times in these suitable days to those with no low-level clouds the data set contains 312 hours of data from 21 suitable days.

2.3. Definition of diagnostics

Diagnostics to compare the model output with the observations of mixed-phase clouds need to be carefully chosen so that they can be equivalently calculated from both modelling and observational datasets. Three diagnostics were chosen that will serve as the method of comparison: water content, cloud fraction and in-cloud water content. Each of these were mean quantities over the whole dataset (described below) and were divided up into temperature ranges each spanning 5°C . The data were averaged over particular temperature ranges because it is expected that microphysical processes such as ice nucleation and deposition growth rate are the important processes in controlling the structure of mixed-phase clouds and these processes are themselves dependent on temperature.

2.3.1. Mean water content

The mean liquid water content and mean ice water content were our primary chosen diagnostics. This is the mean water content observed from the whole dataset, including times when no cloud is observed. This is an important diagnostic because it is a physical quantity directly comparable to the model water contents and because it is an important factor in calculations of radiative exchange. It also has the advantage that, as a dataset mean, it is not sensitive to the resolution of the data and is not dependent on making any other assumptions to make the model data comparable with observations.

2.3.2. Mean cloud fraction

The mean liquid cloud fraction and mean ice cloud fraction were calculated from the whole dataset. Like the mean water content, this quantity is not sensitive to the resolution of the data used. The observed liquid and ice cloud fractions were calculated using the fraction of points in the dataset where the target classification reports the presence of liquid or ice respectively. The classification uses the radar and lidar measurements to determine the most likely object detected. Following *Illingworth et al.* [2007], points where the lidar was unable to detect anything due to attenuation by lower altitude clouds were not included but additional points were added at the top of liquid-layers where the lidar has been attenuated within the liquid-layer but the radar observations indicate the cloud extends higher than this and is likely to contain liquid.

Models typically only have a single cloud fraction quantity which applies to both liquid and ice cloud and this can make comparison to the observations difficult. In some models (e.g. the Met Office Unified Model) the liquid and ice cloud fractions are calculated separately and then combined to create a single value. The Unified Model uses a minimum overlap assumption for liquid and ice clouds which means that the liquid and ice clouds are assumed to fill different parts of the grid-box when the total cloud fraction is less than 1. Therefore the liquid and ice cloud fractions are added together to obtain the total cloud fraction, assuming this gives a value not greater than 1. The liquid and ice cloud fractions can therefore be calculated separately using the model water contents and these values were used in the comparisons. Other models calculate a single cloud fraction from the total condensed water content regardless of phase and determine the ratio of liquid to ice water content later. In these cases it is not possible to determine how much of the cloud fraction comes from liquid and ice or whether it is all mixed-phase. It is therefore assumed that the liquid and ice were maximally overlapped and uniformly mixed throughout the cloudy part of the grid-box and this allows us to use the cloud fraction value output from the model for both the liquid and ice cloud fractions in our comparisons.

2.3.3. Mean in-cloud water content

The mean in-cloud liquid water content and mean in-cloud ice water content were simply the mean of in-cloud water contents calculated by dividing the mean water content in each grid-box by the cloud fraction. This enables us to determine whether modelled clouds had the correct ratio of liquid water to cloud fraction. This quantity is the most sensitive to the resolution chosen because, for instance, a single small cloud passing over the observation site will have a high mean liquid water content when present, but when averaged to the scale of a model grid-box has a cloud fraction below 1 and a lower grid-box mean liquid water mixing ratio. Dividing these quantities for a single cloud will give the same result regardless of resolution; however, this scenario becomes more complicated if a second cloud occurs within the same grid-box but with different properties.

3. Evaluation of operational models

3.1. Operational numerical models

A number of NWP and regional climate models (RCMs) will be compared later and their ability to predict mixed-phase clouds analysed. Table 1 shows details of the model resolution, which ranges between 12 and 79 km in the horizontal and 397 and 636 metres in the vertical at 5 km altitude. As the models are being compared over a long period, where the model has changed, the initial value is given and the most recent value is given in brackets. The table also gives details about the cloud scheme used in each model, the prognostic variables used and the coldest temperature at which liquid water is permitted to exist.

Only two of the models have a cloud scheme where cloud ice is a prognostic variable separate from liquid (UKMO-Meso and UKMO-Global). The other models have a single prognostic variable for total condensed water in the cloud and the ratio of liquid and ice in each grid-box is a diagnostic function of temperature. At warmer temperatures the condensate is mostly liquid transitioning to mostly ice at colder temperatures. This simplification does not allow the models with the diagnostic liquid and ice split to capture the structure of mixed-phase clouds that are observed with liquid occupying the coldest part of the cloud [*Marsham et al.*, 2006].

3.2. Mixed-phase cloud verification

Figure 2 shows the three cloud quantities described in section 2.3 for both the liquid and the ice phase from observed cloud derived from radar and lidar observations and also from a number of NWP forecast models, regional climate models and the ERA-Interim reanalyses. Each of these are plotted as a function of temperature, with the observed quantities being the mean of the observations after they have been averaged on to the numerous model grids and the shaded area represents the range of these observations at that temperature.

The observations of mixed-phase clouds show that, on average, for the 21 days analysed, the mean liquid water content for temperatures between 0 and -20°C is roughly constant with temperature with a value between $1.6\text{--}2.1 \times 10^{-3} \text{ g m}^{-3}$ depending on the model grid chosen. For temperatures colder than -20°C the mean liquid water content decreases exponentially until at -40°C there is virtually no liquid water observed. The observed liquid cloud fraction shows a peak at around -18°C with a maximum cloud fraction of 5.7% whereas the in-cloud liquid water content decreases steadily with decreasing temperature from a value of 0.11 g m^{-3} at 0°C to 0.011 g m^{-3} at -40°C .

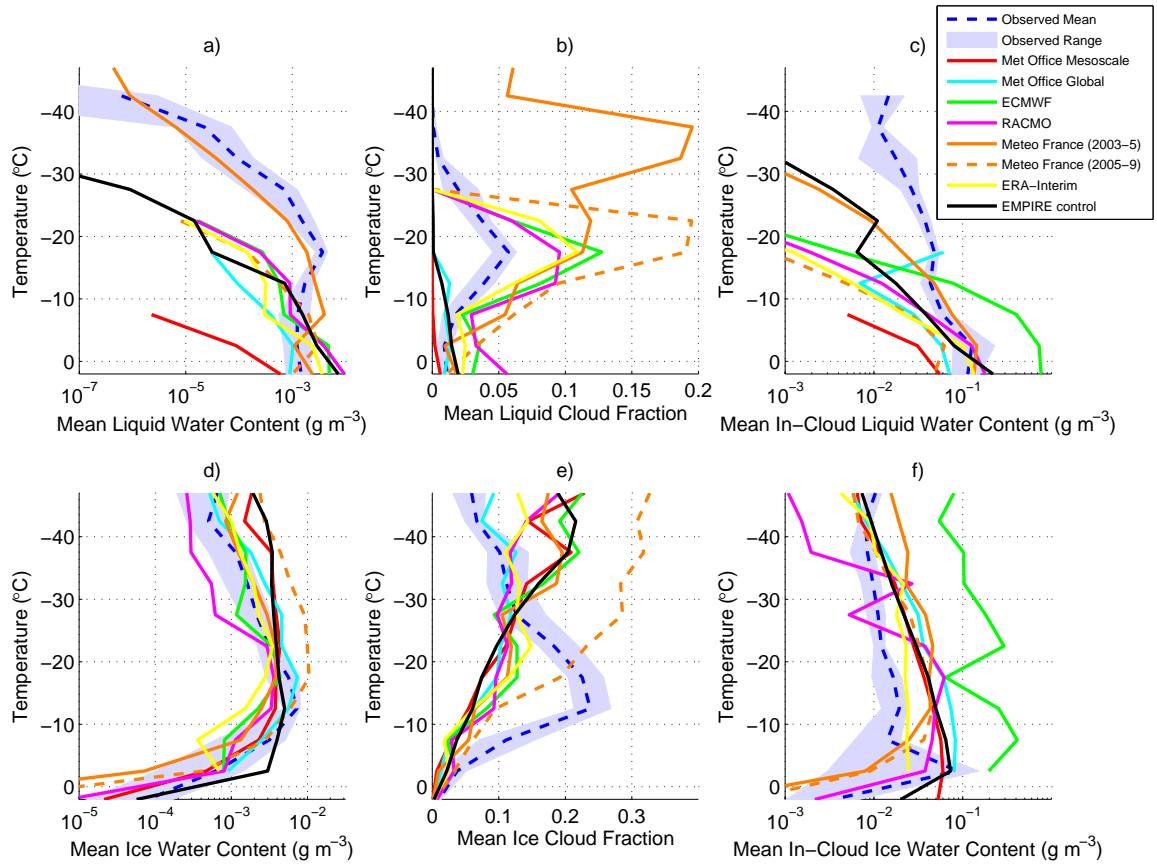


Figure 2. Mean liquid and ice cloud properties from radar and lidar observations and also from a number of NWP forecast models, regional climate models and ERA-Interim reanalyses. These data were for the selected 21 days where mixed-phase clouds or clear skies were observed, each plotted as a function of temperature.

Table 1. Details of the numerical models and their cloud schemes used in later comparisons. Values in brackets show the values used in the model at the end of the comparison period if different to the initial value. Modified from *Illingworth et al. [2007]*.

	UKMO-Meso	UKMO-Global	ECMWF	Météo-France	RACMO	ERA-Interim
Horizontal Resolution (km)	12	60	40 (25)	23.4	18	79
Number of Vertical Levels	38	38	60 (91)	41 (60)	40	60
Grid-box depth at 5 km (m)	615	636	551 (397)	491	523	548
Minimum Liquid Temperature (°C)	-40	-40	-23	-40(-23)	-23	-23
Prognostic Cloud Variables ¹	q_t, q_i	q_t, q_i	q_c, A	q_c	q_c, A	q_c, A

¹Prognostic cloud variables are q_t – total water mixing ratio (vapour + liquid), q_c – cloud (liquid + ice) water mixing ratio, q_i – ice water mixing ratio and A – cloud fraction.

The observations of the ice phase show a maximum in mean ice water content ($7.4 \times 10^{-3} \text{ g m}^{-3}$) and a peak in the ice cloud fraction (23.7%) at -12°C . This peak in the ice water content is around 5°C warmer than the peak in the liquid cloud fraction as might be expected given the typical structure of mixed-phase clouds with a thin liquid layers atop a thicker ice layer. The mean in-cloud ice water content is fairly constant with changing temperature for temperatures colder than -5°C at around 0.02 g m^{-3} .

In terms of the liquid water clouds this analysis shows a number of differences between observed clouds and those simulated by the models. All models underestimate the mean supercooled liquid water content at temperatures below -15°C . The worst performing model is the Met Office Mesoscale model which has no liquid at temperatures colder than -10°C . The Météo France (2003-5) model is the best performer and lies within the range of observations for tem-

peratures between -15°C and -40°C , albeit on the extreme low side of this range. This model, like most models analysed here, uses a diagnostic scheme to determine the ratio of liquid and ice cloud condensate based on the temperature, but is the only diagnostic scheme that allows liquid to exist at temperatures as cold as -40°C . Other diagnostic schemes have a different temperature limit beyond which liquid is not able to exist; in this sample all other models with a diagnostic ratio of liquid and ice do not permit liquid at temperatures below -23°C .

The Météo France (2003-5) model has a much higher mean liquid cloud fraction than the observations, particularly at the colder temperatures, the worst example being a predicted liquid cloud fraction of 19.5% at -37°C where the maximum of the observations at this temperature is only 0.02%. From 2006 onwards the model changed so that the minimum temperature at which liquid can exist was -23°C .

This brought the model in line with other diagnostic models and improved the prediction of liquid cloud fraction, but this also reduced the total liquid water content and showed an underestimate similar to other models.

The two domains of the Met Office Unified Model (mesoscale and global model) are particularly interesting as they are the only models in which ice water content is a prognostic variable separate from liquid. At temperatures warmer than -10°C the predicted liquid water content is just 4.5% (mesoscale) and 62.7% (global) of that observed whereas most other models overestimate the liquid water content at these temperatures. Model performance is worse at colder temperatures with no liquid at temperatures colder than -10°C in the mesoscale model and -20°C in the global model. These were the two models with the least amount of liquid water and the lowest mean liquid cloud fraction. This is an important point; the *Wilson and Ballard* [1999] microphysics scheme used in the Met Office Unified Model is a collection of physically-based parameterizations of the microphysical process rates. The fact that this parameterization scheme results in a severe underestimation of the supercooled liquid water highlights the fact that either these parameterizations are not accurate in the case of mixed-phase clouds, or that other processes not included in the model must be involved in the maintenance of mixed-phase clouds. The poorer performance of this physically-based parameterization compared to the temperature-dependent split of liquid and ice used by other models highlights the importance of further study of the applicability of similar ice microphysics schemes to mixed-phase clouds.

The model predictions of the ice phase were somewhat better than for liquid with the models spanning the range of observations throughout the temperature range analysed. The ice cloud fraction, however, is too large for all models at temperatures colder than -30°C by as much as 0.1, double the observed value. At warmer temperatures all models underpredict the ice cloud fraction and at -12°C the mean observed cloud fraction was 23.4% but the multi-model mean was only 7.3% and the largest model value was 9.5%. The cluster of model predicted ice cloud fractions is remarkably tight given how different they were from the observations.

There are two possible explanations for this absence of ice cloud at -15°C , one being that the models fail to predict ice cloud at this temperature often enough and the other being that the model predicts too little cloud fraction when it does predict cloud. This implies that either the clouds are not forming often enough, or that when they do form they are dissipating too rapidly. The models, except ECMWF and RACMO, diagnose the cloud fraction from the cloud water content.

4. EMPIRE model description

A new model is developed to Evaluate Mixed-Phase Importance in Radiative Exchange and is called EMPIRE. This model is a single column model, designed to be similar to general circulation models (GCMs) used for numerical weather prediction and climate simulations. This enables any potential model improvements identified to be applicable to current models. Comparisons of the process rates with those of large eddy simulations of mixed-phase clouds (shown later, Figure 3) show the model simulates these clouds similarly.

The main advantage of EMPIRE is its flexibility, allowing the model resolution and physics to be easily changed. The default model vertical resolution (50 m) is finer than would be typical of a GCM (around 500 m) and is uniformly spaced through the depth of the troposphere. Additionally it has a non-local vertical diffusivity scheme based on the *Lock et al.*

[2000] boundary layer scheme for stratocumulus, which operates in statically unstable regions where cloud top radiative cooling is occurring; separate diffusivity profiles can be applied to different cloud layers if multiple layers exist. The model is initialised with vertical profiles from ERA-Interim and is forced with advective tendencies derived from ERA-Interim. This advective forcing dataset gives 3-hourly increments of temperature, moisture, and horizontal wind speeds resulting from horizontal advection.

The physics of the model is based on the Met Office Unified Model, including the radiation scheme [*Edwards and Slingo*, 1996], mixed-phase microphysics scheme [*Wilson and Ballard*, 1999], local [*Louis*, 1979] and non-local vertical diffusion [*Lock et al.*, 2000], and cloud scheme [*Smith*, 1990]. The model is described in greater detail below.

As the mixed-phase clouds being modelled are at mid-levels in the troposphere it is also assumed that they are not affected by surface processes on the timescale of a day. Therefore, for simplicity, the surface temperature is prescribed for the duration of the model simulation. This may lead to some biases near the surface, but these are expected to be unimportant in our representation of mixed-phase clouds. Any ice that falls to the melting level is assumed to turn to rain and fall to the surface instantly.

In EMPIRE, θ_l , the liquid-water potential temperature and q_t , the total water mixing ratio are used. These were chosen as they are both conserved within reversible moist adiabatic processes [*Betts*, 1973]. The total water mixing ratio, q_t , is the sum of the water vapour mixing ratio and the liquid water mixing ratio ($q_t = q_v + q_l$). It is assumed that liquid water evaporates and condenses rapidly when present in comparison to the model timestep and therefore the division between q_v and q_l can be treated diagnostically. Each timestep an iterative method is used to convert θ_l and q_t to T , q_v , and q_l . Ice sublimates more slowly than liquid and therefore a prognostic variable to account for the growth of ice is required. EMPIRE also has prognostic variables for the zonal and meridional horizontal windspeed (u , v) to improve accuracy of vertical diffusion calculations.

Ice production in mixed-phase clouds is the main factor that determines how long the liquid persists. There are three different factors that are important for defining how much ice is produced; these are: nucleation, depositional growth and sedimentation. Other microphysical processes, such as ice-rain interactions, rain production and ice multiplication are thought to be unimportant in stratiform mixed-phase clouds and are therefore not included in EMPIRE. The ice scheme is consistent with *Wilson and Ballard* [1999] although with the explicit assumptions about ice crystal habit, terminal velocity and mass-diameter able to be changed freely. *Wilson and Ballard* (and EMPIRE) assume an exponential distribution of sizes based on temperature and ice water content.

Following *Wilson and Ballard*, ice is nucleated every time step within a grid-box when the following conditions are satisfied:

1. At temperatures colder than -40°C , if liquid is present, then all liquid is converted instantly to ice.
2. Heterogeneous nucleation occurs in a grid-box if there is liquid present and the temperature is colder than -10°C .

The number of ice crystals nucleated follows the *Fletcher* [1962] relation, but limited to a maximum value, as used in *Wilson and Ballard* [1999]:

$$n = \min [0.01 \exp(-0.6T), 10^5], \quad (1)$$

where n is the number of ice crystals activated per cubic metre at temperature $T(^{\circ}\text{C})$. Each ice crystal nucleated is given an initial mass of 1×10^{-12} kg. The size of the initial nucleated mass is not important in the model simulations

as the depositional growth term dominates the ice particle growth once it has formed.

Growth by deposition is the primary way that small ice particles can grow. The growth of a single ice particle by vapour diffusion can be calculated following this equation from *Rogers and Yau* [1988]

$$\frac{dm}{dt} = \frac{4 \pi C F S_i}{\left(\frac{L_s}{R_v T} - 1\right) \frac{L_s}{K T} + \frac{R_v T}{e_i(T) D}}, \quad (2)$$

where m is the mass of the ice crystal in kg, C is the capacitance of the ice particle in m, dependent on its size and shape, F is the ventilation coefficient, S_i is the supersaturation of the air with respect to ice, L_s is the latent heat of sublimation, K is the thermal conductivity of air, D is the diffusivity of water vapour in air and e_i is the saturated vapour pressure over ice. The ventilation coefficient is computed as $F = 0.65 + 0.44 \text{Sc}^{1/3} \text{Re}^{1/2}$ [*Pruppacher and Klett*, 1978] with the Schmidt number ($\text{Sc} = 0.6$) and the Reynolds number ($\text{Re} = v(D)\rho D/\mu$) where $v(D)$ is the fall-speed of the ice particle and μ is the dynamic viscosity of air. The temperature dependence of L_s , K and D are neglected; EMPIRE uses values suitable for 0°C , which are $L_s = 2.83 \times 10^6 \text{ J kg}^{-1}$, $K = 2.40 \times 10^{-2} \text{ J m}^{-1} \text{ s}^{-1} \text{ K}^{-1}$ and $D = 2.21 P^{-1} \text{ m}^2 \text{ s}^{-1}$, where P is the air pressure in Pascals. The total growth rate of ice in a grid-box is calculated by applying (2) to each ice particle. This involves integrating over an assumed distribution of ice particle sizes:

$$\left. \frac{dq_i}{dt} \right|_{\text{deposition}} = \frac{1}{\rho} \int_0^\infty \frac{dm}{dt} N_{\text{ice}}(D) dD, \quad (3)$$

where $N_{\text{ice}}(D)$ is the number of ice particles of diameter, D , in metres given by the Wilson and Ballard size distribution as:

$$N_{\text{ice}}(D) = N_{\text{oice}} \exp(-\Lambda_{\text{ice}} D), \quad (4)$$

where

$$N_{\text{oice}} = 2.0 \times 10^6 \exp(-0.1222T), \quad (5)$$

in units of m^{-4} and T is the temperature in degrees Celsius. Λ_{ice} is defined as

$$\Lambda_{\text{ice}} = \left[\frac{\text{IWC}}{a N_{\text{oice}} \Gamma(b+1) \exp(-0.1222T)} \right]^{-\frac{1}{b+1}} \quad (6)$$

where IWC is the ice water content in kg m^{-3} , Γ is the gamma function and a and b are the coefficient and exponent in the mass-diameter relation ($m = aD^b$). The mass (kg) of an ice crystal is related to its diameter (metres) through $m = aD^b$, where $a = 0.0185$ and $b = 1.90$ from *Brown and Francis* [1995].

Ice crystals are assumed to fall at their terminal velocity, which is assumed to be related to the diameter in a similar way to the mass by $V = 25.2D^{0.527}$. The transfer of ice from grid level to grid level is calculated using the mass weighted fall speed and uses the same assumed size distribution as for the ice growth. Ice is not permitted to fall more than one grid level in a timestep.

Radiative transfer in EMPIRE is calculated using the *Edwards and Slingo* [1996] radiation code. Within the radiation scheme the effective radius of liquid droplets is set to $10 \mu\text{m}$ and the effective radius for ice crystals is set to $50 \mu\text{m}$. The radiation scheme also includes the effects of water vapour, ozone, carbon dioxide, methane, oxygen, nitrous oxide and CFCs. By default the radiation scheme is called every 15 minutes throughout the simulation so that the model is able to react quickly if cloud forms. GCMs

typically call the radiation scheme less frequently than this, typically about every 3 hours for climate models, and since mixed-phase clouds are thought to be largely driven by the radiative cooling from cloud top this could be one reason why GCMs do not represent mixed-phase clouds well.

In EMPIRE the sub-grid variability of q_t is parameterized following *Smith* [1990]. This is the cloud scheme used by the Met Office models before July 2010 and still used in limited area model domains. This scheme assumes a triangular distribution of total water mixing ratio within the grid box and the fraction of the grid-box in which cloud exists and the liquid water mixing ratio of the cloud that is present is calculated from this distribution. EMPIRE uses a fixed value of $\text{RH}_{\text{crit}} = 0.85$ for all model levels.

The prognostic equations are solved using a fully implicit scheme for the time derivative and a centred scheme for spatial derivatives, for both the advection and diffusion terms. A tridiagonal solver is used to solve all grid-levels simultaneously. The only exception to this is the ice sedimentation scheme which is solved using a Total Variation Diminishing [TVD, e.g. *Sueby*, 1984] advection scheme. A TVD scheme is used to give an accurate representation of the ice sedimentation which preserves gradients and has minimal numerical diffusion. This cannot be achieved with conventional advection schemes. This is particularly important as it is expected that the formation and sedimentation of ice is a large factor in the depletion of liquid water from mixed-phase clouds.

Grid-box mean liquid and ice water contents from the EMPIRE simulations for 3 July 2003 are shown in Figure 1g,h and agree well with the observed liquid and ice water contents in terms of timing and altitude. The structure of the mid-level mixed-phase cloud simulated is consistent with observed altocumulus clouds, with liquid occupying the coldest part of the cloud and is persistent over several hours.

4.1. Forward modelling of observations

Many of our observations of mixed-phase clouds come from instrumented sites where surface based radar, lidar and microwave radiometers give information about cloud structure. These instruments do not provide perfect information about the clouds present due to the way that they work. For instance, the lidar signal can be fully attenuated by liquid water and therefore any clouds above that height cannot be sampled by the lidar. In addition, the radar sensitivity decreases with distance from the instrument and thus cirrus clouds with low reflectivity, high in the troposphere are not detected. To allow fair comparison between these observations and EMPIRE simulations, radar and lidar forward models are applied to the EMPIRE output. This means taking the model output and sampling the cloud fields (ice and liquid water content) as if they were seen by a radar and lidar. By doing this any potential biases of unsampled clouds are removed and this also allows us to directly compare model output with radar and lidar observations for case studies.

The radar forward model is constructed using an expression from *Hogan et al.* [2006]. This provides ice water content IWC (g m^{-3}) as a function of 35 GHz radar reflectivity factor Z (dBZ) and temperature T ($^\circ\text{C}$). Inverting the relationship yields

$$Z = \frac{\log_{10}(\text{IWC}) + 1.63 + 0.0186T}{2.42 \times 10^{-4}T + 0.0699}. \quad (7)$$

The minimum detectable signal for a radar decreases following the inverse square law. For the 35 GHz radar at Chilbolton the minimum detectable signal (in dBZ) is given by

$$Z_{\text{min}} = -45 + 20 \log_{10} r, \quad (8)$$

where r is the radial distance from the radar antenna in kilometres. The same constraint on the minimum detectable signal is also applied to the forward model so that low reflectivity clouds that could not be observed in reality are not included.

The reflectivity in the forward model is only calculated using the model ice water content field and does not include liquid water. This is because it is assumed that the liquid water observed in these supercooled clouds has a small size and as the radar return is proportional to D^6 these small droplets will likely not influence the radar reflectivity predicted from the forward model. The return from rain is not included, as rain is not a prognostic variable in EMPIRE. The effect of attenuation in the radar forward model is neglected because the liquid and ice water contents are low in mixed-phase clouds and therefore the sensitivity will likely have a much larger effect than attenuation.

The lidar forward model predicts the attenuated backscatter coefficient, β' that would be detected by the instrument. This is done following *Marsham et al.* [2006] and briefly described below. The extinction coefficient, α_j is assumed to be

$$\alpha_j = 1.5 \times \frac{WC_j}{\rho_j r_{ej}} \quad (9)$$

where the subscript j refers to the phase of the hydrometeor (liquid or ice), WC is the water content in kg m^{-3} , ρ is the density of liquid or ice and r_e is the effective radius. The effective radius for liquid is held at a constant value of $10 \mu\text{m}$ to be consistent with the radiation scheme, whereas the ice effective radius is calculated from the mean ice particle mass assuming they are spheres with a density of 700 kg m^{-3} following *Rotstayn et al.* [2000].

The backscatter coefficient, β , can be calculated from the extinction coefficient if the lidar ratio, S , is known. A value of $S = 18.5 \text{ sr}$ is assumed for both liquid and ice as in *Marsham et al.* [2006]: $\beta_j = \frac{\alpha_j}{S_j}$. β is summed across both liquid

and ice species and then the attenuated backscatter coefficient averaged over a layer of thickness Δz is calculated using

$$\beta' = \beta \exp(-2\eta\tau) \frac{1 - \exp(-2\eta\alpha\Delta z)}{2\eta\alpha\Delta z}, \quad (10)$$

where τ is the optical depth of hydrometeors between the lidar and the base of the model level being calculated, defined as

$$\tau = \int_0^z \alpha \, dz, \quad (11)$$

and η accounts for multiple scattering of the lidar beam [*Platt, 1973*] which is approximated as 0.7 for the Chilbolton lidar [*O'Connor et al., 2004*]. The fraction on the right hand side of (10) accurately deals with the attenuation within the layer being calculated [*Hogan, 2006*] where Δz is the depth of the model layer.

5. Importance of modelled physical processes

This section addresses the physical processes in EMPIRE that are important in maintaining mixed-phase clouds. Firstly, the processes that contribute most to the creation and removal of supercooled liquid water in these clouds is assessed. This information is used to identify potential areas of sensitivity to the model configuration, particularly in the physical parameterizations, leading to a number of perturbed physics simulations investigating which areas of the model could be developed to better improve simulations of mixed-phase clouds.

5.1. Process rates in EMPIRE simulation

The dominant processes in generating and depleting liquid water from mixed-phase clouds are identified using EMPIRE. To do this, an idealised simulation is run with no

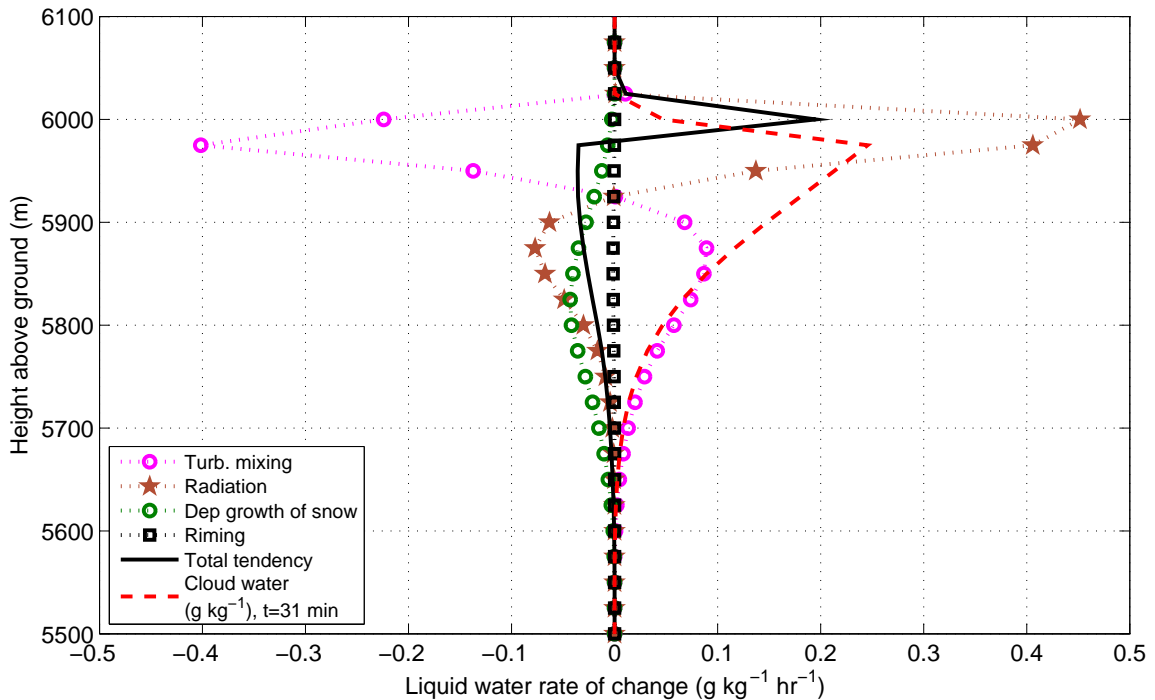


Figure 3. Process rates for EMPIRE simulation of mixed-phase cloud averaged over an hour. The red dashed line shows the liquid cloud water content at the beginning of this time period in units of g kg^{-1} .

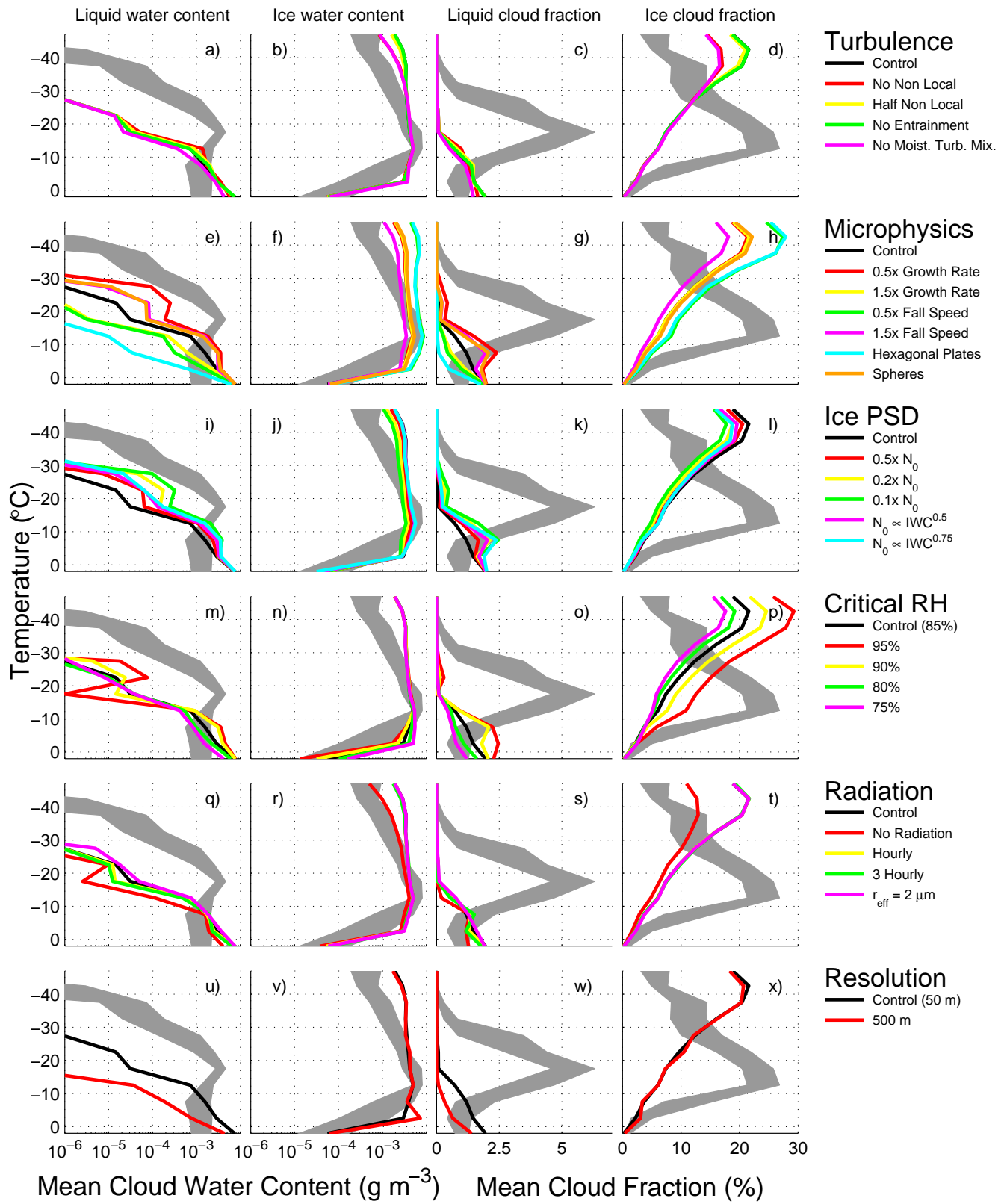


Figure 4. Sensitivities in EMPIRE to changes to the model parameters. Each column is labelled at the top with the diagnostic. Each row represents changes to a family of parameters, the type of which is described on the right of that row. The coloured lines in each row represent the same simulations, as labelled in the legend to the right, but the colours are reused in each row. The black line, showing the control simulation, and the gray shading, showing the range of observations, are the same on each row, as in Figure 2.

vertical velocity but otherwise the model contains all the standard physics described in section 4. The vertical resolution for the idealised experiment is improved from 50 to 25 metres. The model is initialised from a radiosonde sounding from Larkhill at 0600 UTC on 05 September 2003 and then run for 30 minutes to allow the cloud to reach equilibrium. During the following 60 minutes the change to the liquid water content is calculated from each process at each vertical level during each timestep. The average tendency from this 60 minute period is shown as a function of height in Figure 3 together with the profile of liquid water content after 31 minutes, denoted by the red dashed line. The black line represents the average total tendency over the 60 minute period, a sum of all the tendencies.

During the simulation the radiative cooling at cloud top contributes most to the production of liquid water ($+0.45 \text{ g kg}^{-1} \text{ h}^{-1}$) but turbulent mixing near the cloud top reduces the liquid water content ($-0.40 \text{ g kg}^{-1} \text{ h}^{-1}$) by mixing the radiatively cooled air with warmer air lower in the cloud. Lower in the cloud the turbulent mixing acts as a source of liquid water, by enhancing the upward transport of water vapour and the downward transport of radiatively cooled air which increases the total water mixing ratio and reduces the saturation mixing ratio. The radiative impact on the cloud at this level is a weak warming as the absorption by the ice particles is larger than the cooling, resulting in a negative tendency for liquid water. Ice growth by deposition increases with depth from the cloud top with the growth rate related to the ice water content. The net result of all of these processes is a slight reduction ($-0.03 \text{ g kg}^{-1} \text{ h}^{-1}$) in the amount of liquid water throughout the depth of the cloud, largely related to the depositional growth of ice particles. However, at the cloud top, at and above the height of maximum liquid water content there is an increase in the amount of liquid water ($+0.20 \text{ g kg}^{-1} \text{ h}^{-1}$), caused by radiative cooling but unlike lower in the cloud the cooled air is not mixed with warmer air lower in the cloud by turbulent mixing. This results in the increasing tendency at the cloud top and as the simulation evolves this leads to an increase of cloud top height with time.

These findings agree well with those of [Smith *et al.*, 2009, their Figure 8] who used large-eddy simulations to assess the process rates in mixed-phase clouds. The process rates are of roughly equal magnitudes to the process rates from EMPIRE, but the main difference is that the increasing liquid water content at cloud top is largely a result of large scale ascent whereas in this EMPIRE simulation there is no large scale ascent and the increasing tendency is caused by an offset in the location of the maximum cooling and peak in the turbulent mixing.

5.2. Sensitivity to perturbing physics in EMPIRE

The importance of changes to the physics in EMPIRE is assessed in this section. Changes to the model liquid and ice water contents are assessed, together with the cloud fraction of each phase. Differences in liquid and ice water content between simulations are quoted as changes to the mean at temperatures between -10°C and -30°C . At temperatures colder than -30°C the liquid water content is negligibly small and the ice water content is too large relative to observations, whereas at temperatures warmer than -10°C the liquid water is greater than observations and shows relatively little sensitivity to change in the ice microphysics as ice is not nucleated until the temperature is -10°C or colder.

Figure 4 shows the sensitivity to many different model parameters. Each row shows changes to one family of parameters, the type described on the right hand side. The gray shaded area shows the range of observed values as in Figure 2, the black line shows values from the EMPIRE control simulations and the coloured lines represent the perturbed

physics simulations. The same coloured lines on each row relate to the same set of simulations, but colours are repeated on different rows showing different sets of simulations.

The first row of Figure 4 shows the sensitivity of cloud properties to changes in the specification of sub-grid turbulence. Sensitivity experiments included halving the non-local mixing, turning it off completely and letting the local mixing scheme do the work and turning off cloud top-entrainment. There is remarkably little sensitivity to the specification of turbulent mixing in EMPIRE, much less than for other model changes described below, which is surprising given the important role the turbulent mixing has on redistributing the liquid, ice and vapour (Fig. 3). The biggest increase in the liquid water content occurs when the non-local mixing is turned off for all variables as this prevents ice being mixed from lower in the cloud towards the cloud top. In contrast the largest decrease in liquid water content occurs when the non-local mixing of the total water content (q_t) is turned off in isolation as this removes the source of vapour to be condensed at the top of the cloud layer.

The second row details the changes resulting from alterations to the microphysical processes affecting ice growth rate and fall speed. This shows the largest sensitivity in terms of mean liquid water content of all the perturbed physics experiments. The largest increases, roughly equal in magnitude, are when the capacitance of the ice particles is reduced by 50% or their fall velocity is increased by 50%. The largest decrease in liquid water content is found when the capacitance is increased or the fall velocity decreased. The ice particle habit is an important factor determining both its capacitance and fall speed as a function of size so the preferred habit is also important; where hexagonal plates are assumed, the liquid water content is lowest. This is because hexagonal plates have an increased capacitance and reduced fall velocity relative to the aggregates assumed as default.

The sensitivity of changing the intercept parameter (N_0) of ice particle size distribution is shown in the third row, which also has a large effect on the mean liquid water content. The reason for the large sensitivity is because changing the size distribution changes the relative contribution of small and large ice particles in a grid-box and therefore changes both the ice growth and sedimentation rates calculated. By decreasing N_0 for low ice water contents we increased the mean size of the ice particles and consequently the total growth by deposition of the particles is reduced and the average mass-weighted fall velocity is increased. As we saw in the above microphysics sensitivities, both of these changes increased the mean liquid water content. This sensitivity to size distribution will be explored further in section 6.

Unsurprisingly, the cloud water contents and cloud fractions can be changed by altering the scheme that diagnoses cloud fraction, as can be seen in the fourth row of Figure 4. By varying the critical relative humidity at which cloud forms (RH_{crit}) the amount of cloud present in the simulations is modified. Surprisingly, it is an increase in RH_{crit} , and requiring the model grid-box to be more humid before forming cloud, that increases the mean liquid water content, whereas reducing RH_{crit} reduces the cloud water content. This is exactly opposite of what would happen if one changed RH_{crit} instantaneously in the model. This curious result can be explained by considering a grid box with a mean humidity just in excess of RH_{crit} , with a low cloud fraction and small quantity of condensed water. As ice particles form in the grid box and grow by vapour deposition, they remove much of the liquid water. In a similar simulation with higher RH_{crit} it required higher q_t before any cloud forms, but when it does, the liquid water content and

cloud fraction are higher for the same excess humidity. The ice production and growth by deposition is slightly more efficient as the supersaturation over ice is higher, but because liquid is diagnosed initially it takes longer for all the liquid to be removed and is therefore more likely to be present when the radiation scheme is next called. If it is still present then a cloud top cooling will be diagnosed which will aid in the maintenance of the liquid water in the layer.

The sensitivity to radiation is shown in row five. Turning the radiation scheme off completely reduces the mean liquid water content by 85.1% compared to the control simulation, which recalculates the radiative fluxes every 15 minutes. Decreasing the frequency that the radiation scheme is called reduces the liquid water content by an average of 10% if called once per hour and 34% if called once every three hours. The sensitivity to radiation timestep is caused by liquid clouds forming and then glaciating between radiation scheme updates, resulting in the cloud top cooling not being captured. GCMs typically call the radiation scheme every one to three hours and this could explain part of the underestimate of modelled supercooled liquid. However, this effect is of smaller magnitude than the sensitivity to ice microphysics described above.

A large sensitivity to vertical grid spacing is shown in the bottom row of Figure 4 where coarser resolution simulations with 500 metre grid spacing have 95% less liquid water, at temperatures below -10°C , than simulations with 50 metre grid spacing. This is a key reason why models with ice water content as a separate prognostic variable fail to simulate enough supercooled liquid water. The GCMs studied here have vertical grid-spacings of between 397–636 m at an altitude of 5 km (Table 1). Climate models typically have coarser vertical (and horizontal) resolution than the GCMs we have studied. The reasons behind the vertical resolution sensitivity are examined in part II of this paper but pertain to unresolved vertical structure of the cloud layer towards the top of the cloud.

In summary, the EMPIRE model shows there is a sensitivity to many different model parameters, most significantly to the implementation of ice microphysics. There are also sensitivities to RH_{crit} , radiation timestep and turbulent mixing specification although the latter 2 are less significant. The sensitivity to vertical grid spacing is the most striking sensitivity and likely a key reason state-of-the-art forecast models still fail to capture mixed-phase clouds correctly.

6. Ice particle size distribution

There is considerable sensitivity to the model ice particle size distribution (Fig. 4i–l). In this section, the standard *Wilson and Ballard* [1999] parameterization is compared with aircraft size spectra data from the European Cloud and Radiation Experiment (EUCREX) field campaign. Figure 5 shows the ratio of process rates calculated from the parameterized size distribution, based on T and IWC alone, to those calculated from the aircraft size spectra. Ice particle growth rates are compared in panels a–c and mass-weighted fall velocity in panels d–f. The ratios are plotted as a function of ice water content (IWC) for individual size spectra in dots, and the mean ratio within each IWC bin is shown in the black dashed line. Values in excess of 1 show the parameterization is producing ice growth rates or fall velocities that are too large.

For small ice water contents typical of mixed-phase clouds, the default parameterization of *Wilson and Ballard* [1999] (eq. 5, where $N_{0\text{ice}}$ is a function of temperature alone) shows a large overestimate of the ice growth rate (Fig. 5a) and a large underestimate of the mass-weighted fall velocity (Fig. 5d). This appears to be a result of the ice particle size

distribution being too steep, with too many small ice particles and too few large ones. The total number concentration of the distribution can be modified by changing the intercept parameter, N_0 . Reducing N_0 for small ice water contents and increasing it for large IWC reduces the biases. Two different functions for N_0 are tested, based on the observed relationships of *Delanoë and Hogan* [2008] and *Morrison et al.* [2011]. The relationship in *Delanoë and Hogan* [2008] is approximately $N_0 \propto \text{IWC}^{0.5}$ whereas *Morrison et al.* [2011] analysed aircraft observations of Arctic mixed-phase clouds during SHEBA and found a slightly stronger relationship of $N_0 \propto \text{IWC}^{0.627}$. N_0 is modified to be a function of IWC,

$$N_0 = 2.0 \times 10^6 \exp(-0.1222T) \times \left(\frac{\text{IWC}}{10^{-2}}\right)^A \text{ m}^{-4} \quad (12)$$

where IWC is in g m^{-3} and A has been set to a value of 0.5 (Fig. 5b,e) and 0.75 (Fig. 5c,f). The standard parameterization is obtained with $A = 0$.

By modifying the size distribution in this way, biases in the calculated process rates are much reduced, particularly where $A = 0.75$. This correction is slightly larger than suggested by the literature but provides a large reduction in the biases of both growth rate and fall velocity over a large range of ice water content values. Including such a modification in EMPIRE simulations, and modifying both fall speed and growth rate accordingly, results in a 134% increase of the mean supercooled liquid water content averaged across all simulations (light blue line in Fig 4i), in much better agreement with observations.

7. Conclusions

This study has evaluated 5 operational models and their ability to simulate mixed-phase altocumulus clouds by comparing their output with data from ground-based remote sensing over 21 days. Additionally, a new single column model, EMPIRE, was created in order to determine how complex models need to be in order to correctly simulate mixed-phase clouds and what improvements could be made to existing models to improve their representation of mixed-phase clouds. The key findings of this study are:

1. Operational models, for the period studied, underestimated supercooled liquid water content by at least a factor of 2.
2. The models with the most sophisticated ice microphysics schemes, and separate prognostic variables for ice and liquid, perform worst of all models and had virtually no supercooled liquid water on the days studied.
3. Any model changes that affect the rate at which ice grows had a large impact on the duration of the mixed-phase cloud layer and its water content.
4. High vertical resolution is important if the model is to capture the mixed-phase cloud. Simulations at 500 metre resolution had only 5% of the supercooled liquid water that was present in the 50 metre simulations.
5. Using a fixed value of the intercept parameter in the ice particle size distribution for all ice water contents results in large biases in microphysical processes rates for high and low ice water content values and consequently altocumulus clouds that glaciate too quickly. This can be corrected by introducing a proportionality of N_0 on IWC^A , where A is between 0.5 and 0.75, based on aircraft observations.

6. There appears to be no need to introduce prognostic ice nuclei to remedy the representation of mixed-phase clouds in large-scale models.

The factor-of-2-underestimate of supercooled liquid water content is rather concerning especially given that models with the most advanced mixed-phase microphysics are the worst performing models. These models with a separate ice

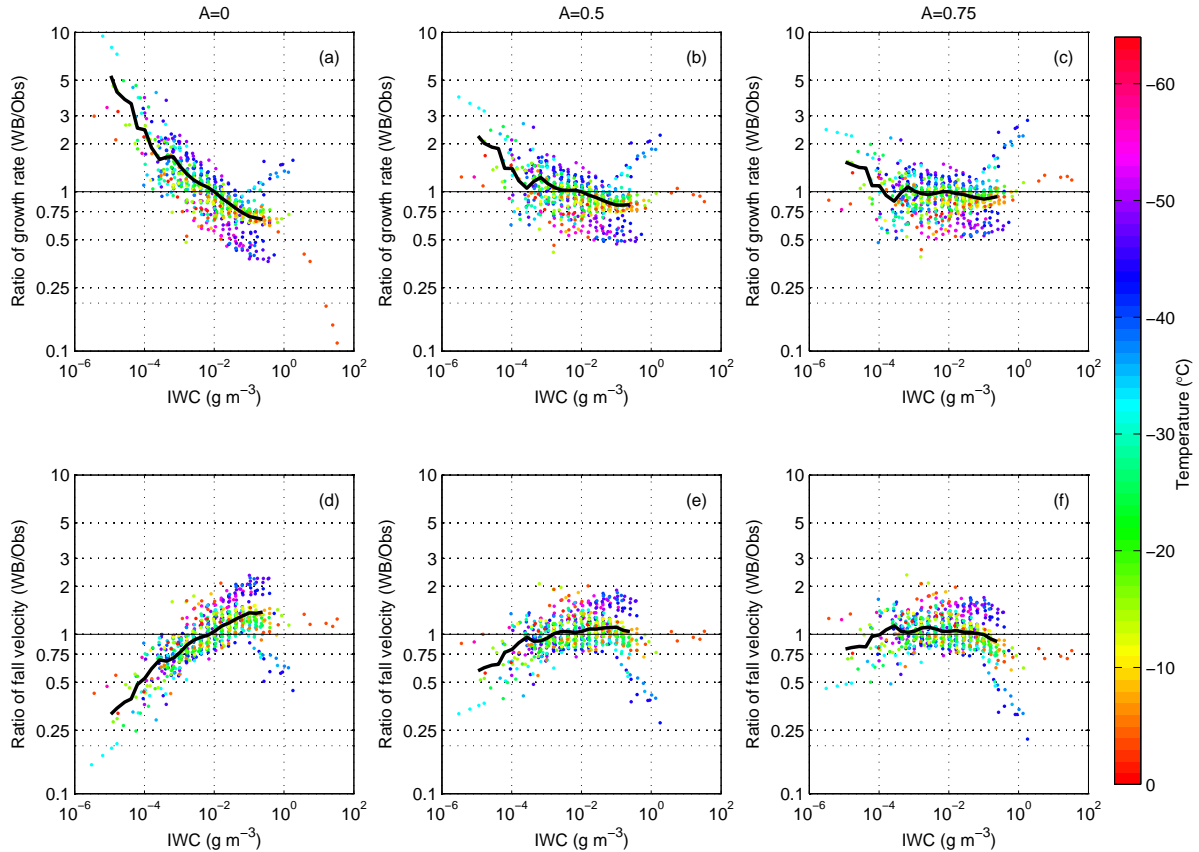


Figure 5. The parameterized process rates from *Wilson and Ballard [1999]* plotted as a fraction of the true growth rate calculated using size distributions observed during EUCREX. Panels a-c show the growth rates and panels d-f show fall velocities. This is shown as a function of ice water content (x-axis) and temperature (colour) for the standard parameterization (panels a and d) and two modifications of the size distribution with $N_0 \propto \text{IWC}^A$ (panels b, c, e and f). Each coloured dot represented an single aircraft size distribution and the black line shows the mean value in each ice water content bin.

prognostic variable seem unable to maintain any supercooled liquid water in their mixed-phase clouds. In contrast, the simpler models without a separate prognostic variable for ice are not capable of representing the liquid-over-ice structure that is observed. Both of these model types will likely present substantial radiative biases on certain days due to these problems.

By implementing changes to the model physics in EMPIRE, it was found that mixed-phase clouds are sensitive to anything that changes the ice growth rate, whether that be directly by changing the capacitance or indirectly by changing the fall speed, habit or size distribution of ice particles. Less significant (but not insignificant) sensitivities to the interval between successive calls of the radiation scheme and the critical relative humidity at which cloud forms in the model were also found. EMPIRE showed little sensitivity to the specification of sub-grid turbulent mixing in the vertical, a surprising result given the importance of the turbulent mixing in controlling the vertical structure of mixed-phase clouds (Fig. 3). There is also a large sensitivity to the vertical grid spacing of the model. Simulations with a vertical grid spacing of 500 metres had only 5% of the liquid water at temperatures below -10°C compared to the simulations performed with 50 metre vertical grid spacing. This results from the profiles of cloud properties at cloud top not being resolved in the coarse model simulations, an area which is discussed in greater detail in the Part II of this paper.

The lifetime of mixed-phase altocumulus clouds is underestimated using the standard ice particle size distribution

from [*Wilson and Ballard, 1999*]. Large biases in both the ice growth rate and the ice fall speed occur for small ice water content values, typical of mixed-phase altocumulus, when using the size distribution because it has a fixed value of N_0 . The size distribution has too many small ice particles and too few large ones when compared to observed size spectra. The model therefore calculates growth rates that are too fast and fall speeds that are too slow; both effects act to increase the ice growth rate and therefore decrease the liquid depletion rate. The biases can be removed across a large range of ice water content values by using an ice particle intercept parameter that varies as a function of ice water content; doing so removes much of the low bias compared to observations, increasing the mean simulated supercooled liquid water content by 134%.

Mixed-phase altocumulus clouds occur when the balance of cloud-top cooling, ice production, turbulent mixing and large-scale ascent produce a cloud where the rate of change of supercooled liquid water with time is near to or above zero. We found that changes to any of these processes produced changes of the cloud supercooled liquid water content but that changes that increase the rate of ice production reduce the amount of liquid present by the largest amount. Microphysics is therefore important in determining the evolution of these cloud systems but accurate microphysics alone is not sufficient; all processes must be simulated sufficiently well. Coarse vertical resolution is one example that prevents these processes being simulated accurately and Part II of this paper [*Barrett et al., 2014*] investigates the causes of the vertical resolution sensitivity more

thoroughly and develops a parameterization of the vertical structure of mixed-phase altocumulus clouds for use in large-scale models so as to remove the resolution sensitivity.

Acknowledgments. The first author was supported by a PhD studentship from the Natural Environment Research Council (NERC). We thank Stephen Belcher and Daniel Kirshbaum for useful discussions throughout the course of this work and Paul Field for his insights on many aspects of this research. We are very grateful to Roel Neggers and Martin Köhler for providing and assisting with the ERA-Interim advective tendencies.

References

- Andrews, T., J. M. Gregory, M. J. Webb, and K. E. Taylor (2012), Forcing, feedbacks and climate sensitivity in CMIP5 coupled atmosphere-ocean climate models, *Geophys. Res. Lett.*, *39*, L09,712, doi:10.1029/2012GL051607.
- Barrett, A. I., R. J. Hogan, and R. M. Forbes (2014), Why are mixed-phase altocumulus clouds poorly predicted by large-scale models? Part II: Vertical resolution sensitivity and parameterization, *J. Geophys. Res.*
- Betts, A. K. (1973), Non-precipitating cumulus convection and its parameterization, *Q. J. R. Meteorol. Soc.*, *99*, 178–196.
- Bony, S., R. Colman, V. M. Kattsov, R. P. Allan, C. S. Bretherton, J.-L. Dufresne, A. Hall, S. Hallegatte, M. M. Holland, W. Ingram, D. A. Randall, B. J. Soden, G. Tselioudis, and M. J. Webb (2006), How well do we understand and evaluate climate change feedback processes?, *J. Clim.*, *19*, 3445–3482.
- Brown, P. R. A., and P. N. Francis (1995), Improved measurements of the ice water content in cirrus using a total-water probe, *J. Atmos. Oceanic Technol.*, *12*, 410–414.
- Delanoë, J., and R. J. Hogan (2008), A variational scheme for retrieving ice cloud properties from combined radar, lidar and infrared radiometer, *J. Geophys. Res.*, *113*, D07,204.
- Dufresne, J.-L., and S. Bony (2008), An assessment of the primary sources of spread of global warming estimates from coupled atmosphere-ocean models, *J. Clim.*, *21*, 5135–5144.
- Edwards, J. M., and A. Slingo (1996), Studies with a flexible new radiation code. I: Choosing a configuration for a large-scale model, *Q. J. R. Meteorol. Soc.*, *122*, 689–719.
- Fletcher, N. H. (1962), *The physics of rainclouds*, University Press, Cambridge.
- Fridlind, A. M., B. van Dierenhoven, A. S. Ackerman, A. Avramov, A. Mrowiec, H. Morrison, P. Zuidema, and M. D. Shupe (2012), A FIRE-ACE/SHEBA case study of mixed-phase Arctic boundary-layer clouds: Entrainment rate limitations on primary ice nucleation processes, *J. Atmos. Sci.*, *69*, 365–389.
- Gregory, D., and D. Morris (1996), The sensitivity of climate simulations to the specification of mixed phase clouds, *Clim. Dyn.*, *12*, 641–651.
- Hobbs, P. V., and A. L. Rangno (1985), Ice particle concentrations in clouds, *J. Atmos. Sci.*, *42*, 2523–2549.
- Hogan, R. J. (2006), Fast approximate calculation of multiply scattered lidar returns, *Applied Optics*, *45*, 5984–5992.
- Hogan, R. J., P. N. Francis, H. Flentje, A. J. Illingworth, M. Quante, and J. Pelon (2003), Characteristics of mixed-phase clouds: Part I: Lidar, radar and aircraft observations from CLARE’98, *Q. J. R. Meteorol. Soc.*, *129*, 2089–2116.
- Hogan, R. J., M. D. Behera, E. J. O’Connor, and A. J. Illingworth (2004), Estimate of the global distribution of stratiform supercooled liquid water clouds using LITE lidar, *Geophys. Res. Lett.*, *31*, L05,106.
- Hogan, R. J., M. P. Mittermaier, and A. J. Illingworth (2006), The retrieval of ice water content from radar reflectivity factor and temperature and its use in evaluating a mesoscale model, *J. Appl. Meteorol.*, *45*, 301–317.
- Illingworth, A. J., R. J. Hogan, E. J. O’Connor, D. Bouniol, M. E. Brooks, J. Delanoë, D. P. Donovan, N. Gaussiat, J. W. F. Goddard, M. Haefelin, H. K. Baltink, O. A. Krasnov, J. Pelon, J.-M. Piriou, A. Protat, H. W. J. Russchenberg, A. Seifert, A. M. Tompkins, G.-J. van Zadelhoff, F. Vinit, U. Willen, D. R. Wilson, and C. L. Wrench (2007), Cloudnet - continuous evaluation of cloud profiles in seven operational models using ground-based observations, *Bull. Amer. Meteor. Soc.*, *88*, 885–898.
- Klein, S. A., R. B. McCoy, H. Morrison, A. S. Ackerman, A. Avramov, G. de Boer, M. Chen, J. N. S. Cole, A. D. Del Genio, M. Falk, M. J. Foster, A. Fridlind, J.-C. Golaz, T. Hashino, J. Y. Harrington, C. Hoese, M. F. Khairoutdinov, V. E. Larson, X. Liu, Y. Luo, G. M. McFarquhar, S. Menon, R. A. J. Neggers, S. Park, M. R. Poellot, J. M. Schmidt, I. Sednev, B. J. Shipway, M. D. Shupe, D. A. Spangenberg, Y. C. Sud, D. D. Turner, D. E. Veron, K. von Salzen, G. K. Walker, Z. Wang, A. B. Wolf, S. Xie, K.-M. Xu, F. Yang, and G. Zhang (2009), Intercomparison of model simulations of mixed-phase clouds observed during the ARM Mixed-Phase Arctic Cloud Experiment. I: Single-layer cloud, *Q. J. R. Meteorol. Soc.*, *135*(641), 979–1002, doi:10.1002/qj.416.
- Lock, A. P., A. R. Brown, M. R. Bush, G. M. Martin, and R. N. B. Smith (2000), A new boundary layer mixing scheme. Part I: Scheme description and single-column model tests, *Mon. Wea. Rev.*, *128*, 3187–3199.
- Louis, J.-F. (1979), A parametric model of vertical eddy fluxes in the atmosphere, *Bound.-Layer Meteorol.*, *17*, 187–202.
- Marshall, J. H., S. Dobbie, and R. J. Hogan (2006), Evaluation of a large-eddy model simulation of a mixed-phase altocumulus cloud using microwave radiometer, lidar and Doppler radar data, *Q. J. R. Meteorol. Soc.*, *132*, 1693–1715.
- McFarquhar, G. M., S. Ghan, and Coauthors (2011), Indirect and semi-direct aerosol campaign: The impact of arctic aerosols on clouds, *Bull. Amer. Meteor. Soc.*, *92*, 183201, doi:10.1175/2010BAMS2935.1.
- Mitchell, J. F. B., C. A. Senior, and W. J. Ingram (1989), CO₂ and climate: a missing feedback?, *Nature*, *341*, 132–134.
- Morrison, H., P. Zuidema, G. M. McFarquhar, A. Bansemmer, and A. J. Heymsfield (2011), Snow microphysical observations in shallow mixed-phase and deep frontal arctic cloud systems, *Q. J. R. Meteorol. Soc.*, *137*, 1589–1601.
- Morrison, H., G. de Boer, G. Feingold, J. Harrington, M. D. Shupe, and K. Sulia (2012), Resilience of persistent arctic mixed-phase clouds, *Nature Geoscience*, *5*, 11–17.
- O’Connor, E. J., A. J. Illingworth, and R. J. Hogan (2004), A technique for autocorrelation of cloud lidar, *J. Atmos. Oceanic Technol.*, *21*, 777–786.
- Platt, C. M. R. (1973), Lidar and radiometric observations of cirrus clouds, *J. Atmos. Sci.*, *30*, 1191–1204.
- Pruppacher, H. R., and J. D. Klett (1978), *Microphysics of clouds and precipitation*, D. Reidel Publishing Company, Boston, USA.
- Rauber, R. M., and A. Tokay (1991), An explanation for the existence of supercooled water at the top of cold clouds, *J. Atmos. Sci.*, *48*, 1005–1023.
- Rogers, R. R., and M. K. Yau (1988), *A Short Course in Cloud Physics*, Pergamon Press.
- Rotstayn, L. D., B. F. Ryan, and J. J. Kattfey (2000), A scheme for calculation of the liquid fraction in mixed-phase stratiform clouds in large-scale models, *Mon. Wea. Rev.*, *128*, 1070–1088.
- Senior, C. A., and J. F. B. Mitchell (1993), Carbon dioxide and climate: The impact of cloud parameterization, *J. Clim.*, *6*, 393–418.
- Shupe, M. D., J. Daniel, G. de Boer, E. W. Eloranta, P. Kollias, C. N. Long, E. P. Luke, D. D. Turner, and J. Verlinde (2008), A focus on mixed-phase clouds, *Bull. Amer. Meteor. Soc.*, *89*, 1549–1562.
- Smith, A. J., V. E. Larson, J. Niu, J. A. Kankiewicz, and L. D. Carey (2009), Processes that generate and deplete liquid water and snow in thin midlevel mixed-phase clouds, *J. Geophys. Res.*, *114*, D12,203.
- Smith, R. N. B. (1990), A scheme for predicting layer clouds and their water content in a general circulation model, *Q. J. R. Meteorol. Soc.*, *116*, 435–460.
- Sun, Z., and K. P. Shine (1994), Studies of the radiative properties of ice and mixed-phase clouds, *Q. J. R. Meteorol. Soc.*, *120*, 111–137.
- Sweby, P. K. (1984), High-resolution schemes using flux limiters for hyperbolic conservation-laws, *SIAM J. Numer. Analysis*, *21*, 995–1011.
- Tsushima, Y., S. Emori, T. Ogura, M. Kimoto, M. J. Webb, K. D. Williams, M. A. Ringer, B. J. Soden, B. Li, and N. Andronova (2006), Importance of the mixed-phase cloud distribution in the control climate for assessing the response of clouds to carbon dioxide increase: a multi-model study, *Clim. Dyn.*, *27*, 113–126.

- Uttal, T., J. Curry, and Coauthors (2002), Surface heat budget of the arctic ocean, *Bull. Amer. Meteor. Soc.*, *83*, 255275, doi: 10.1175/1520-0477(2002)083;0255:SHBOTA;2.3.CO;2.
- Verlinde, J., J. Y. Harrington, G. M. McFarquhar, V. T. Yanzuzi, A. Avramov, S. Greenberg, N. Johnson, G. Zhang, M. R. Poellot, J. H. Mather, D. D. Turner, E. W. Eloranta, B. D. Zak, A. J. Prenni, J. S. Daniel, G. L. Kok, D. C. Tobin, R. Holz, K. Sassen, D. Spangenberg, P. Minnis, T. P. Tooman, M. D. Ivey, S. J. Richardson, C. P. Bahrman, M. Shupe, P. J. DeMott, A. J. Heymsfield, and R. Schofield (2007), The Mixed-Phase Arctic Cloud Experiment, *Bull. Amer. Meteor. Soc.*, *88*, 177–190.
- Wilson, R. W., and S. P. Ballard (1999), A microphysically based precipitation scheme for the UK Meteorological Office Unified Model, *Q. J. R. Meteorol. Soc.*, *125*, 1607–1636.
- Zhang, D., Z. Wang, and D. Liu (2010), A global view of middle-level liquid-layer topped stratiform cloud distribution and phase partition from calipso and cloudsat measurements, *J. Geophys. Res.*, *115*, D00H13.
- Zhang, M. H., W. Y. Lin, S. A. Klein, J. T. Bacmeister, S. Bony, R. T. Cederwall, A. D. D. Genio, J. J. Hack, N. G. Loeb, U. Lohmann, P. Minnis, I. Musat, R. Pincus, P. Stier, M. J. Suarez, M. J. Webb, J. B. Wu, S. C. Xie, M.-S. Yao, and J. H. Zhang (2005), Comparing clouds and their seasonal variations in 10 atmospheric general circulation models with satellite measurements, *J. Geophys. Res.*, *110*, D15S02.

Corresponding author: Andrew. I. Barrett, Department of Meteorology, University of Reading, Reading, RG6 6BB, UK. (a.i.barrett@reading.ac.uk)